Comparative analysis of cellular structures in fresh and dehydrated tropical fruits using confocal microscopy

A. Espeleta-Maya[1], J. Martínez-Trinidad[2], L. Moreno-Pacheco[2] and R. A. García-León[3]*

[1]Facultad de Ingenierías, Grupo de Investigación GIEEP, Universidad del Magdalena, Santa Marta, Colombia, [2]Grupo Ingeniería de Superficies, Instituto Politécnico Nacional, Unidad Zacatenco, SEPI-ESIME-ZAC, Mexico City, Mexico, [3]Universidad Francisco de Paula Santander Ocaña, Facultad de Ingeniería, Grupo de investigación INGAP, Ocaña, Colombia

This study quantitatively investigated dehydration-induced microstructural and biochemical transformations in Hass avocado, sugar mango, papaya, and Honey Gold pineapple using confocal laser scanning microscopy (CLSM). The methodology involved comparing fluorescence intensity in fresh and dehydrated tissues and validating these measurements through proximate composition and statistical analysis, including a three-way ANOVA (fruit species × temperature × air velocity). Results showed increased fluorescence in avocado (31%), mango (28%), and pineapple (35%), with strong correlations to protein enrichment ($R^2 > 0.92$), while papaya exhibited a 22% decrease despite higher protein content, suggesting conformational rearrangements that reduced fluorophore accessibility. The ANOVA confirmed that fruit species significantly affected fluorescence intensity and protein content ($p < 0.0001$), temperature had a moderate effect ($p = 0.0112$), and air velocity showed no significant influence ($p = 0.13$). Overall, CLSM proved to be a reliable tool for linking dehydration severity with molecular and nutritional transformations, offering a robust framework for optimizing drying parameters and enhancing the quality preservation of tropical fruits.

KEYWORDS

confocal laser scanning microscopy (CLSM), tropical fruits, dehydration, protein fluorescence, microstructural changes, nutritional quality

1 Introduction

Tropical fruits are among the most valuable agricultural resources worldwide due to their cultural and economic impact and their remarkable nutritional composition. They are significant sources of vitamins (A, C, and E), minerals, dietary fiber, and phytochemicals with antioxidant activity that contribute to the prevention of chronic diseases (Pawley, 1995). Among these, Hass avocado (*Persea americana*), sugar mango (*Mangifera indica*), papaya (*Carica papaya*), and Honey Gold pineapple (*Ananas comosus*) are particularly relevant for tropical and subtropical regions. Their structural complexity—parenchymatic tissues with diverse water content, lipid-rich mesocarp cells in avocado, pectin-rich papaya pulp, and fibrous vascular arrangements in pineapple—directly influences postharvest physiology, shelf life, and consumer acceptability (Heredia and Dominguez, 2009; Yahia, 2011).

Dehydration is one of the oldest and most effective methods of preserving fruits. Reducing water activity inhibits microbial growth, slows enzymatic reactions, and facilitates transportation by lowering weight and volume (Schaffer et al., 2013). However, dehydration is not merely a physical process of water removal: it induces profound microstructural alterations, including cell wall collapse, reduction of intercellular spaces, plasmolysis, and redistribution of intracellular components such as starch granules, lipids, and proteins (Sana et al., 2025). These transformations significantly affect the functional and sensory properties of the final product, including texture, color stability, aroma retention, and rehydration capacity. Furthermore, they determine the extent of nutritional preservation, since bioactive compounds such as carotenoids, polyphenols, and vitamins are often associated with specific cellular compartments (Ratti, 2001). Therefore, understanding these microstructural dynamics is essential to optimize drying technologies that balance efficiency with quality preservation.

Confocal laser scanning microscopy (CLSM) has emerged as a key technique for the structural characterization of plant-based foods, providing non-destructive, three-dimensional visualization of tissues with subcellular resolution. By exploiting autofluorescence and specific fluorophores, CLSM enables the mapping of biomolecules such as proteins, lipids, and cell wall components, while minimizing sample preparation and preserving native microstructures. Compared to electron microscopy, which often requires destructive treatments, CLSM offers the advantage of capturing optical sections in fresh or partially dry samples.

More broadly, fluorescence-based techniques have become increasingly relevant in food science for monitoring physiological changes, assessing compositional attributes, and classifying products during postharvest and processing stages. Their non-invasive nature, combined with the integration of advanced data analysis tools, has expanded their utility for extracting detailed information from biological tissues. Within this context, CLSM stands out as a powerful approach to investigate the cellular responses of tropical fruits to dehydration, a process in which microstructural alterations directly affect sensory, nutritional, and preservation qualities (Galeano-Díaz et al., 2025).

1.1 Related works

Drying is one of the most widely applied preservation techniques for tropical and subtropical fruits, as it reduces water activity, extends shelf life, and facilitates commercialization. However, the choice of drying method strongly influences the physicochemical and functional properties of the final product, including sugar content, amino acid profile, color, and the extent of non-enzymatic browning. In the case of Chilean papaya (*Vasconcellea pubescens*), different drying methods, including freeze-drying, vacuum drying, solar drying, convective drying, and infrared drying, have been investigated to evaluate their effects on product quality and biological functionality. These studies emphasize that drying modifies sensory and nutritional attributes and can affect bioactive compounds with potential implications for human health. Thus, understanding how operational parameters modulate microstructural and biochemical changes during papaya dehydration is crucial to optimize processing strategies that balance quality preservation with functional benefits (Vega-Gálvez et al., 2021).

Sando et al. (2009) conducted a histochemical study on the laticifer structure of *Hevea brasiliensis*, employing spectral confocal laser scanning microscopy to enhance the visualization of rubber particle formation and distribution. Their findings revealed that laticifer networks initially develop through anastomoses but later rupture due to radial division and ray growth. Immunohistochemical analyses also showed that the small rubber particle protein (SRPP) is explicitly localized in conducting phloem laticifers. In contrast, the rubber elongation factor (REF) is distributed across all laticifer layers, highlighting their distinct roles in rubber biosynthesis (Sando et al., 2009).

Onelli et al. (2016) analyzed the softening mechanisms in melting flesh (MF) and non-melting flesh (NMF) peaches, focusing on the biomechanical properties of the exocarp and mesocarp, as well as the localization of phenolic compounds, including flavonoids and hydroxycinnamic acids. Their study demonstrated that cell wall dismantling and turgor loss in MF fruits shifted firmness control to the epidermis. In contrast, in NMF fruits, the mesocarp cell wall integrity played a decisive role in maintaining firmness (Onelli et al., 2016).

Vega-Gálvez et al. (2021) conducted a comprehensive study on *Parmentiera edulis* (cuajilote), characterizing its cellular architecture, physicochemical composition, and micromechanical properties at different maturity stages. Their findings highlighted significant changes in cellulose and lignin content associated with ripening, as well as structural modifications in sclerenchyma fibers that influence the mechanical performance of the fruit (Vicente-Flores et al., 2021).

Recent advances in microscopy and imaging have further expanded the understanding of food microstructure. For instance, Qiang et al. (2025) developed a novel 3D microscopy system with specialized software that enabled precise quantification of fruit cell geometry. Their study on tomatoes and strawberries at different ripening stages revealed variations in cell diameters of up to 29.7%, demonstrating the importance of microstructural analysis in assessing fruit physiology and postharvest quality (Hongli et al., 2025).

1.2 Aim of this work and research gap

Tropical fruits grow in warm regions between the Tropic of Cancer and the Tropic of Capricorn, covering nearly 40% of the Earth's surface and sustaining about half of the world's plant families. Countries in these regions, particularly South America and Southeast Asia, account for most global production. Among the wide variety of tropical fruits, avocado, mango, papaya, and pineapple are of outstanding economic and nutritional relevance, driving growth in both fresh consumption and processed markets such as canned fruit, freeze-dried products, and beverages (Zhang et al., 2025). These fruits are valued for their sensory and nutritional attributes and for their diverse seed and core structures, which differ in weight proportions and chemical composition. Such variability directly influences their functional potential, including the presence of proteins, polysaccharides, and bioactive compounds.

Although confocal laser scanning microscopy (CLSM) has become increasingly used in food science, most reported applications have focused on model plant tissues, ripening dynamics, or emulsified systems (Mohapatra and Mishra, 2011). Very few studies have investigated dehydration-induced microstructural transformations in

tropical fruits, and even fewer have quantitatively linked fluorescence changes to biochemical composition. This lack of integrative analyses limits the optimization of dehydration processes specifically adapted to tropical matrices.

Compared to other microscopy techniques such as SEM, TEM, or Cryo-SEM, CLSM offers distinct advantages: it allows non-destructive, three-dimensional imaging of hydrated or partially dehydrated tissues, preserving native microstructure without fixation artifacts; it enables quantitative fluorescence detection that can be directly related to biomolecular localization (e.g., proteins, lipids, and polysaccharides); and it facilitates the correlation of microstructural visualization with compositional or functional data. These attributes make CLSM particularly suitable for assessing the effects of dehydration on cellular integrity and the preservation of nutrients in plant-based foods. This work is novel in applying CLSM as a quantitative and comparative tool to directly evaluate microstructural and biochemical responses to dehydration in four tropical fruits (Hass avocado, Sugar mango, papaya, and Honey Gold pineapple). The study aims to bridge the current methodological and interpretative gaps by linking confocal fluorescence data with proximate composition analyses, thereby providing quantitative evidence of how dehydration conditions influence protein distribution and conformational accessibility at the cellular level. Also, it is hypothesized that protein-associated fluorescence intensity, as detected by CLSM, correlates with dehydration severity (temperature and airflow) and aligns with the proximate protein content expressed on a dry-weight basis. Also, some objectives are derived from the aim: (i) To visualize dehydration-induced microstructural alterations using CLSM; (ii) To quantify fluorescence intensity and correlate it with proximate protein content; and (iii) To compare species-specific structural responses to dehydration to better understand the relationship between microstructure and nutritional composition.

1.3 Knowledge gaps and research opportunities

The literature review highlights critical limitations of using CLSM in the study of dehydrated tropical fruits: (1) Absence of systematic comparative studies between fresh and dried tissues. (2) Methodological difficulties in sample preparation, including partial rehydration, altered autofluorescence, and limited fluorochrome penetration. And (3) Lack of standardized protocols, hindering reproducibility across research groups. Future opportunities lie in developing specialized sample-preparation protocols for dehydrated matrices and in incorporating advanced image analysis approaches, such as fractal dimension analysis, 3D porosity quantification, and evaluation of intercellular connectivity.

2 Materials and methods

2.1 Data analysis

The extracted data included information on the microscopic techniques employed, the structural parameters evaluated, the primary findings, and the methodological limitations. These were compared with confocal laser scanning microscopy (CLSM) images

obtained from fresh fruit samples and from samples dehydrated by forced convection at controlled air velocity and specific dehydrator temperatures, as shown in Figure 1. Proximate chemical analyses of the fruits, before and after dehydration, were also conducted to establish correlations between protein content and fluorescence intensity.

2.2 Proposed methodological framework

A comprehensive methodological framework was established to integrate standardized sample preparation, controlled drying conditions, and quantitative microscopic and statistical analysis to investigate the microstructural and biochemical effects of dehydration on tropical fruits. The experimental workflow is summarized schematically in Figure 2. The methodology comprised the following steps:

Step 1—sample selection and preparation: Fruits (Hass avocado, sugar mango, papaya, and Honey Gold pineapple) were selected at a uniform ripening stage and free from mechanical damage to ensure consistency in texture, chemical composition, and water content. Each fruit was weighed before processing to determine fresh mass. After washing, peeling, and deseeding, only the edible pulp was retained and weighed again to calculate edible yield. The Pulp of each fruit was sliced into 6–8 mm-thick sections to standardize dehydration rates and minimize variability caused by differences in surface area and diffusion path length. Fruits were sourced from local suppliers in Colombia (2025 harvest, at commercial maturity). All fruits were visually inspected and selected for uniform ripeness and absence of defects. For each fruit species, 10 independent biological replicates ($` = 10$) were analyzed. Each replicate corresponded to a distinct fruit specimen, and all subsequent slices from that fruit were treated as technical subsamples.

Step 2—dehydration process: Prepared slices were placed on stainless-steel trays inside a forced-convection dehydrator. Tray tare weights were recorded to precisely monitor water loss. Temperatures of 50, 60, and 70 °C were chosen to represent moderate-to-high convective drying conditions frequently used in studies assessing fruit quality while limiting excessive thermal degradation. Air velocities of 2.0 and 4.0 m s^{-1} were selected to provide contrasting convective mass-transfer conditions and to evaluate the effect of airflow on drying kinetics and microstructural integrity. These parameter ranges have been widely employed in convective drying and process-optimization experiments on fruit matrices (Rasooli Sharabiani et al., 2021; Tejeda-Miramontes et al., 2024; Panarese et al., 2012). However, temperature and air velocity ranges were intentionally varied to generate comparative dehydration conditions, allowing the evaluation of microstructural and compositional changes under mild to moderate convective intensities representative of industrial drying environments.

Weight measurements were recorded every 10 min using an analytical balance (ME204T; precision ± 0.01 g). Moisture content (wet basis) at time t was calculated as: $MC_{wet}(t) = \dfrac{m_t - m_{dry}}{m_t} \times 100\%$,

where m_t is the sample mass at time t and m_{dry} is the mass after oven-drying to constant weight (70 °C; Hass avocado ≈ 8 h, mango ≈ 13 h,
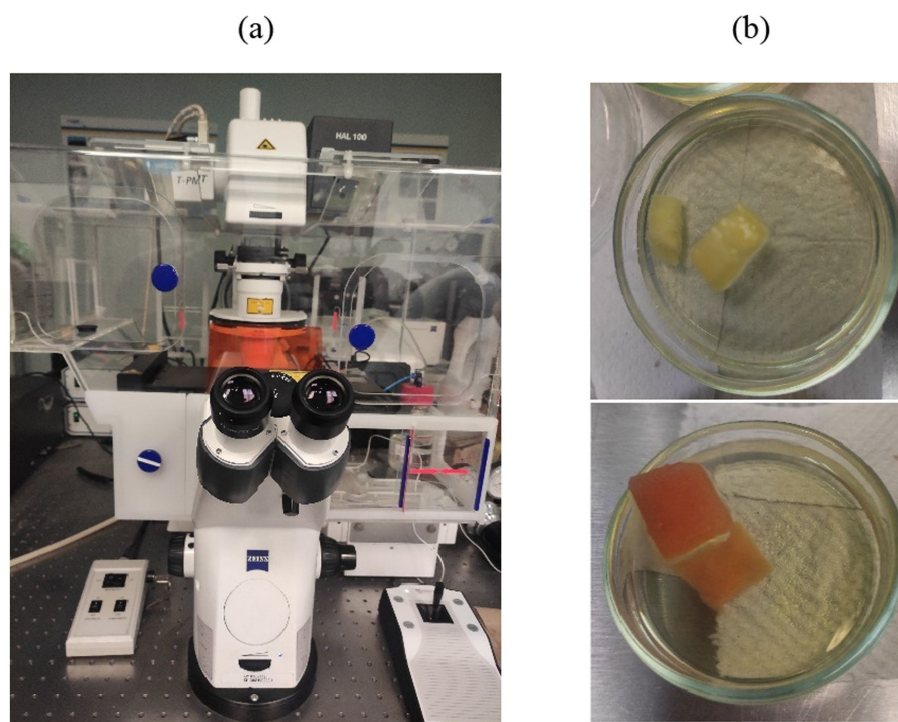
FIGURE 1
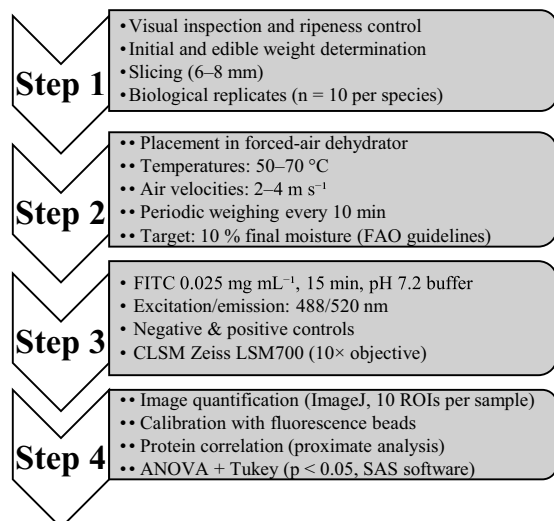(a) Confocal microscope, and (b) Fruit samples.

Step 1
• Visual inspection and ripeness control
• Initial and edible weight determination
• Slicing (6–8 mm)
• Biological replicates (n = 10 per species)

Step 2
•• Placement in forced-air dehydrator
•• Temperatures: 50–70 °C
•• Air velocities: 2–4 m s⁻¹
•• Periodic weighing every 10 min
•• Target: 10 % final moisture (FAO guidelines)

Step 3
• FITC 0.025 mg mL⁻¹, 15 min, pH 7.2 buffer
• Excitation/emission: 488/520 nm
• Negative & positive controls
• CLSM Zeiss LSM700 (10× objective)

Step 4
•• Image quantification (ImageJ, 10 ROIs per sample)
•• Calibration with fluorescence beads
•• Protein correlation (proximate analysis)
•• ANOVA + Tukey (p < 0.05, SAS software)

FIGURE 2
Schematic experimental workflow summarizing the main stages of the study.

papaya ≈ 17 h, pineapple ≈ 20 h). Proximate composition values were converted to a dry-weight basis using MC_{dry} and expressed as g per 100 g dry matter. A final moisture content of approximately 10% (wet basis) was targeted to obtain shelf-stable dried fruits, ensuring low water activity and comparability with previous FAO guidelines (Fautsch Macías, 2014).

Step 3—FITC staining and histological preparation: Histological sections (1–2 mm) were obtained from both fresh and dehydrated samples, minimizing tissue damage. Protein localization was achieved using fluorescein isothiocyanate (FITC). The staining procedure was optimized by testing dye concentrations (0.01–0.05 mg mL⁻¹) and incubation times (10–20 min). Optimal results were obtained at 0.025 mg mL⁻¹ for 15 min, providing high signal-to-noise ratios and minimal background. After incubation, samples were rinsed with phosphate-buffered saline (pH 7.2) to remove unbound dye, then mounted in glycerol for observation.

Fluorescence was detected using a Zeiss LSM700 confocal laser scanning microscope with a 10 × objective (NA 0.3), excitation wavelength 488 nm, and emission collection at 520 nm. Acquisition parameters were standardized across all species: Avocado: Gain 838, Gamma 1.19, Offset −41.28; Mango: Gain 883, Gamma 1.20, Offset −64; Papaya: Gain 933, Gamma 1.10, Offset −30; Pineapple: Gain 1,020, Gamma 1.10, Offset −42. Images (512 × 512 px, 850 μm × 850 μm field) satisfied Nyquist sampling requirements for accurate spatial resolution. For fluorescence validation, FITC-negative controls (unstained tissue) and FITC-positive controls (protein-rich avocado mesocarp) were analyzed to confirm the absence of autofluorescence artifacts and dye specificity. Quantification was performed in ImageJ (NIH, USA) using 10 regions of interest (ROIs) per image. Calibration was performed using reference fluorescence beads (Invitrogen F8810) to ensure linearity between intensity and emission response.

Moisture, protein, lipid, and ash contents were determined following standard AOAC procedures (Baur and Ensminger, 1977) as part of the proximate composition analysis. Moisture content was measured by oven-drying at 105 °C to constant weight

according to AOAC Official Methods (925.10; 930.15). Although high-sugar fruits may be sensitive to elevated temperatures, samples were dried in thin layers and monitored to constant weight, preventing sugar degradation and ensuring complete removal of free and bound water for a standardized dry-mass basis. Protein content was determined by the Kjeldahl method (N × 6.25). All measurements were performed in triplicate and expressed on a dry-weight basis.

Step 4—statistical and data analysis: All statistical analyses were performed using SAS software, version 9.4. The experimental design followed a three-way factorial design (4 fruit species × 3 drying temperatures × 2 air velocities), with 10 biological replicates ($n = 10$) per fruit species. Data normality and variance homogeneity were verified using the Shapiro–Wilk and Levene tests, respectively. A three-way ANOVA (General Linear Model procedure, PROC GLM) was applied to assess the effects of *fruit species*, *drying temperature*, and *air velocity*, as well as their interactions, on fluorescence intensity and protein content (dry-weight basis). When significant effects were detected, Tukey's Honest Significant Difference (HSD) test was performed for multiple comparisons at a significance level of $p < 0.05$. Tukey HSD test was applied on least square means (LSMeans) adjusted by the GLM model.

The Pearson correlation coefficient (r) between mean fluorescence intensity and protein content was computed using the PROC CORR procedure to evaluate the strength and direction of the relationship, and the coefficient of determination (R^2) was used to describe the degree of linear association. All data are reported as mean ± standard deviation (SD).

2.3 Application of confocal microscopy in tropical fruits

Confocal laser scanning microscopy (CLSM) in tropical fruits remains limited; however, its ability to reveal cellular-level structural transformations makes it a promising tool for postharvest and dehydration studies. Existing literature highlights preliminary applications in fruit ripening and tissue characterization, though systematic analyses comparing fresh and dehydrated tissues are lacking. Then, in Table 1, the conditions for each fruit are described in detail. On the other hand, protein localization was achieved using fluorescein isothiocyanate (FITC), a protein-specific fluorophore. Samples were incubated with FITC for 15 min, rinsed to remove unbound dye, and mounted in an appropriate medium for CLSM observation.

3 Results and discussion

3.1 Quantification of protein content and fluorescence intensity

Figure 3 provides a detailed overview of the mean fluorescence intensity in fresh and dehydrated tropical fruits for $n = 10$ replicated by sample conditions. In contrast, Table 2 complements this information by reporting the proximal chemical composition. Together, these datasets reveal consistent patterns and highlight
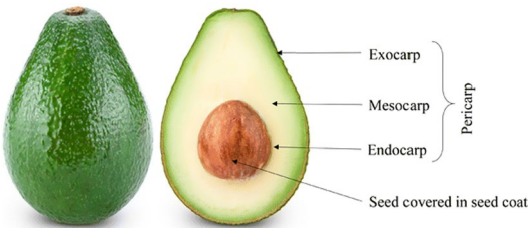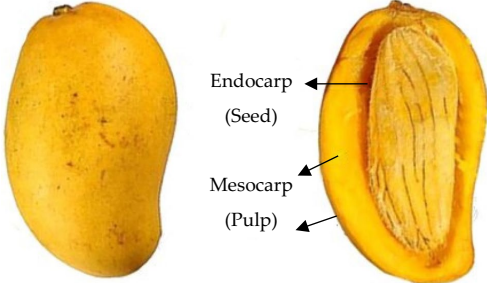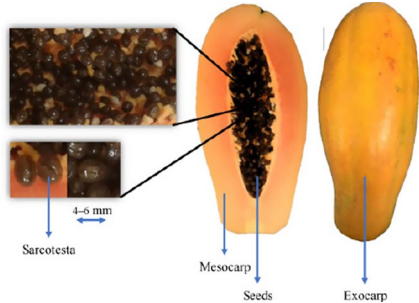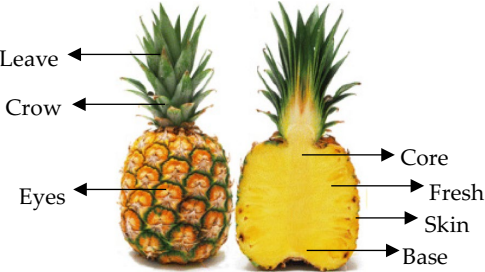
species-specific deviations, shedding light on the complexity of dehydration effects.

The results reveal that dehydration led to an overall increase in protein content across all fruits, confirming the expected concentration effect associated with water removal. This trend was reflected in the fluorescence intensities of avocado, mango, and pineapple, suggesting a direct correlation between protein concentration and fluorescence. Specifically, avocado and mango demonstrated the most pronounced changes: avocado increased from 2.00 to 6.74% protein, accompanied by a fluorescence rise from 24.98 to 61.76; mango rose from 0.50 to 2.73% protein, with fluorescence jumping almost 25-fold (1.30 to 32.44). Pineapple showed a more moderate response, with fluorescence rising from 25.92 to 38.68 and proteins from 0.53 to 3.32%. However, papaya represents a notable exception. Despite an increase in protein content (0.61 to 4.90% on a dry-weight basis), its fluorescence intensity decreased from 80.19 to 66.72. This behavior may be linked to protein aggregation, altered residue accessibility, or matrix effects that reduce probe binding. These explanations remain hypotheses that require confirmation with complementary techniques such as FTIR, DSC, or CD. This result highlights that fluorescence intensity cannot be interpreted solely as a function of biomolecule concentration; instead, it must be understood in the context of the surrounding structural and biochemical environment.

Note that statistical analysis indicated that the fluorescence and compositional trends were consistent across the tested drying temperatures and air velocities. This suggests that the observed structural effects were primarily species-dependent rather than condition-dependent within the studied range. All differences in fluorescence intensity and protein content between fresh and dehydrated samples were statistically significant ($p < 0.05$), and the data showed good reproducibility across independent replicates. The relatively high standard deviation observed in mango and papaya samples can be attributed to their intrinsic biological heterogeneity, variable cellular density, uneven fluorochrome penetration, and minor differences in autofluorescence background. These factors are inherent to heterogeneous plant matrices analyzed by CLSM. Possible optical artifacts, including photobleaching, were minimized by maintaining uniform laser power, scan speed, and exposure time, and by limiting image acquisition to a single optical pass per region of interest (ROI). Negative controls confirmed the stability of background fluorescence, ensuring that intensity variations reflected actual biochemical or structural differences rather than optical noise.

Table 2 provides additional insights by comparing the chemical composition of fresh and dehydrated samples. As expected, moisture content dropped dramatically in dehydrated fruits (73–91% to below 15%), concentrating all other components. Proteins, fats, and carbohydrates exhibited species-dependent increases. In avocado, the fat content rose sharply from 15.00 to 50.43%, indicating that lipids became the dominant macronutrient after water removal. On the other hand, mango, papaya, and pineapple exhibited very high carbohydrate concentrations in the dehydrated state (85.53, 79.93, and 84.48%, respectively). These differences suggest that the nutritional profile of dehydrated fruits diverges significantly, with avocado becoming a protein–lipid-rich matrix, while mango, papaya, and pineapple become carbohydrate-dominant.

TABLE 1 Fruit considerations.

| Fruit and description	Main parts
Hass avocado (*Persea americana*): CLSM has primarily been used to investigate ripening processes in avocado, with autofluorescence signals arising from lignin, chlorophylls, and anthocyanins. Structurally, the fruit consists of a thin epicarp (peel), a thick mesocarp (pulp), and a single large endocarp (seed coat surrounding the seed). The mesocarp, rich in lipids and proteins, is the main edible portion and undergoes significant softening and biochemical changes during ripening. Despite advances in characterizing ripening-related autofluorescence, no comparative studies have been conducted between fresh and dehydrated tissues, leaving a gap in understanding dehydration-induced modifications in the mesocarp microstructure (Magwaza and Tesfay, 2015).	
Mango (*Mangifera indica*, "Sugar" variety): Microscopy-based approaches have described varietal differences and ripening dynamics in mango, focusing on changes in cell density, intercellular spaces, and vascular tissue distribution within the mesocarp. The fruit comprises a leathery epicarp, a fibrous and succulent mesocarp (pulp), and a woody endocarp enclosing the seed. These structures strongly influence water diffusion during dehydration, particularly the fibrous mesocarp that contain starch, sugars, and phenolic compounds. Although CLSM can potentially reveal changes in protein localization and cellular integrity during drying, studies directly addressing dehydration-induced modifications remain limited (Choudhary et al., 2023).	
Papaya (*Carica papaya*): Research in papaya has mainly relied on SEM and FT-IR, showing alterations in the cell wall, particularly pectin degradation, as the main factor behind softening during ripening. Morphologically, papaya consists of a smooth epicarp, a voluminous mesocarp forming the edible pulp, and a central cavity containing numerous seeds enclosed in mucilaginous sarcotesta. The mesocarp is rich in water, carotenoids, and proteins, making it highly susceptible to structural collapse during dehydration. However, CLSM applications in papaya, especially for dehydrated tissues, are virtually absent, offering an opportunity to deepen understanding of protein conformational changes and microstructural integrity during drying (Ovando-Martínez and González-Aguilar, 2020).	
Pineapple (*Ananas comosus*, "Honey Gold" variety): Studies on pineapple are scarce and have primarily focused on general ripening-related structural aspects. Pineapple is a composite fruit formed by the fusion of multiple flowers, with a rough epicarp (peel with bracts), a fibrous mesocarp (pulp), a central fibrous core (peduncle), and vascular bundles running longitudinally. These fibrous and highly lignified structures strongly influence drying behavior, as water movement occurs through complex vascular networks. No CLSM-based evaluations of dehydration effects have been reported, despite the technique's potential to provide insight into protein distribution and cell wall integrity during drying (Azizan et al., 2020).	
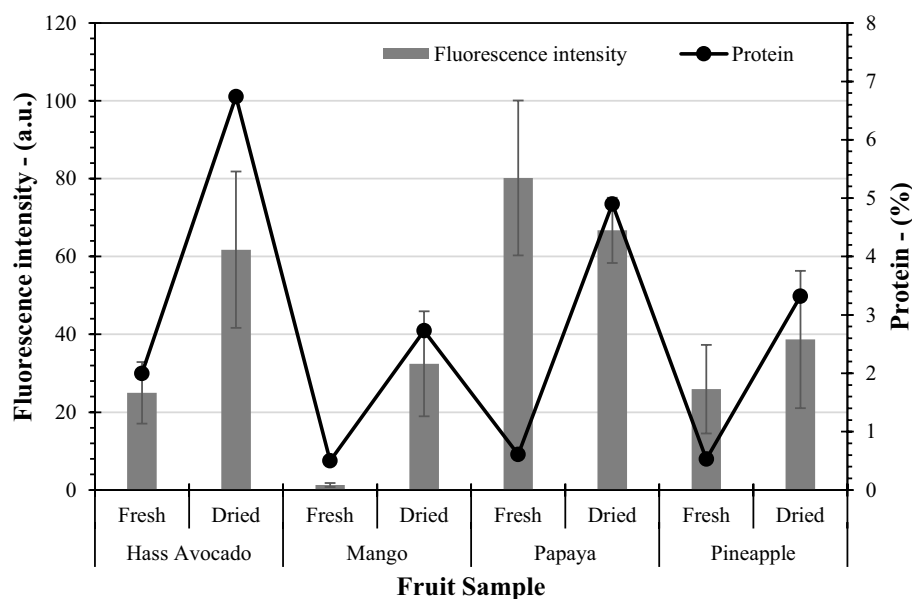
FIGURE 3
Comparison between fluorescence intensity and protein content.

TABLE 2 Proximate chemical content for fresh and dehydrated fruit samples.

Common name	Moisture (%)		Proteins (%)		Lipid (%)		Minerals (%)		CHO's (%)	
	Fresh	Dried	Fresh	Dried	Fresh	Dried	Fresh	Dried	Fresh	Dried
Hass avocado	73.23 ± 5.12		2.00 ± 0.14	6.74 ± 0.47	15.00 ± 1.05	50.43 ± 3.53	0.77 ± 0.05	2.59 ± 0.18	9.00 ± 0.63	30.24 ± 2.12
Mango	79.30 ± 5.55		0.50 ± 0.04	2.73 ± 0.19	0.00 ± 0.00	0.00 ± 0.00	0.40 ± 0.03	1.74 ± 0.12	19.80 ± 1.39	85.53 ± 5.99
Papaya	90.63 ± 6.35	10.00 ± 0.70	0.61 ± 0.05	4.90 ± 0.34	0.24 ± 0.02	2.35 ± 0.17	0.29 ± 0.02	2.82 ± 0.20	8.23 ± 0.58	79.93 ± 5.60
Pineapple	86.01 ± 6.02		0.53 ± 0.04	3.32 ± 0.23	0.12 ± 0.01	0.77 ± 0.05	0.22 ± 0.02	1.43 ± 0.10	13.12 ± 0.92	84.48 ± 5.91

Fruits with higher lipid fractions (e.g., avocado) display stronger fluorescence–protein correlations, possibly because lipids stabilize protein structures during dehydration, maintaining probe accessibility. Note that when both tables are considered together, a coherent pattern emerges. On the other hand, fruits rich in carbohydrates (e.g., papaya) may undergo structural rearrangements, such as sugar–protein interactions or Maillard-type precursors, that reduce fluorescence despite their higher protein content. This interpretation aligns with previous theoretical models (Terai and Nagano, 2008), emphasizing that fluorescence depends not only on biomolecule concentration but also on conformational integrity and the physicochemical environment.

3.2 Statistical analysis results

The ANOVA results (Table 3) revealed a highly significant effect of fruit species ($p < 0.0001$) on both fluorescence intensity and protein content, as well as a moderate but significant influence of temperature ($p = 0.0112$). No significant effect was observed for air velocity alone, but a significant interaction (Species × Temperature, $p = 0.0065$) indicated that thermal sensitivity varied among fruit types. *Post hoc* Tukey's HSD tests ($\alpha = 0.05$) confirmed that avocado differed

significantly from papaya and pineapple ($p < 0.01$), showing higher protein-associated fluorescence due to its lipid-rich matrix. In contrast, mango and papaya showed greater data dispersion, linked to their higher sugar content and autofluorescence variability. Note that no higher-order interactions were observed (Species × Temp × Velocity, $p > 0.05$).

Strong positive correlations between protein content and fluorescence intensity were observed for all species (Table 4), with R^2 values ranging from 0.72 to 0.92, confirming that fluorescence intensity reliably reflects protein content and dehydration severity. These correlations validate CLSM as a quantitative indicator of biochemical concentration and structural preservation across fruit species. Residual analysis confirmed the validity of the statistical model, showing both normality and homoscedasticity (Shapiro–Wilk $p > 0.10$; Levene's test p > 0.05).

3.3 Observations from confocal microscopy images

The confocal microscopy images (Figure 4) visually confirm the quantitative results in Figure 3 and Table 2, enabling

TABLE 3 ANOVA results.

Source of variation	Degrees of freedom (DOF)	F-value	p-value	Significance
Fruit species	3	122.48	<0.0001	$p < 0.001$
Drying temperature	2	4.96	0.0112	$p < 0.05$
Air velocity	1	2.37	0.1314	Not significant
Species × Temperature	6	3.28	0.0065	$p < 0.01$
Species × Air velocity	3	1.72	0.1648	Not significant
Temperature × Air velocity	2	1.05	0.3521	Not significant
Error	72	–	–	–

TABLE 4 Pearson correlation.

| Fruit species	r (protein vs. fluorescence)	R^2	p-value
Avocado	0.95	0.90	<0.001
Mango	0.96	0.92	<0.001
Papaya	0.85	0.72	<0.01
Pineapple	0.93	0.87	<0.001

All correlations are significant at $p < 0.01$.

microstructural interpretation of protein distribution in both the fresh and dehydrated states. The corresponding histograms reflect fluorescence intensity profiles, further supporting the observed differences across species. Then, a detailed description of the fruit samples is presented:

- *Hass avocado:* In fresh avocado tissue, the fluorescence signal appears scattered and of low intensity, as shown by the narrow peak in the histogram centered at lower intensity values. After dehydration, the images reveal a denser, more continuous fluorescence distribution across the cell walls and cytoplasm. The histogram shifts toward higher-intensity values and shows a broader distribution, consistent with the 2.00% → 6.74% increase in protein (Table 2) and the rise in average fluorescence from 24.98 to 61.76 (Figure 3). These results indicate that dehydration concentrates proteins and enhances their accessibility to fluorophores. Also, similar proteins were found by Vilhena et al.(2020).

- *Mango:* Fresh mango tissue displays very weak fluorescence, with most of the signal concentrated in isolated bright spots, reflected in the histogram's low baseline. After dehydration, however, the images exhibit a striking increase in fluorescence, with numerous well-defined and uniformly distributed spherical domains. The histogram shows an expansion across a wider intensity range, consistent with the substantial increases in average fluorescence (1.30 → 32.44) and protein content (0.50% → 2.73%). This suggests that dehydration concentrates proteins and exposes additional binding sites by partially unfolding protein structures.

- *Papaya:* Papaya presents a contrasting behavior. In the fresh state, the images exhibit strong, widespread fluorescence, as reflected in a histogram with a broad, high-intensity distribution. After dehydration, the images reveal a reduction in both fluorescence

intensity and homogeneity (Li et al., 2023). The histogram narrows and shifts toward lower values, despite the protein content rising from 0.61 to 4.90%, a decrease of 17%. This suggests conformational alterations, such as denaturation, aggregation, or sugar-protein interactions, that hinder fluorophore binding.

- This contradiction indicates that dehydration in papaya alters protein conformation or promotes aggregation, hindering fluorophore accessibility. Interactions with sugars and polysaccharides, abundant in papaya and concentrated during dehydration (Figure 3: CHO content increases to ~80%), may further contribute to fluorescence quenching.

- *Pineapple:* Fresh pineapple images show dispersed but moderate fluorescence signals, with the histogram reflecting an intermediate distribution. After dehydration, fluorescence becomes more pronounced and better defined around cell-like structures, and the histogram shifts to higher intensity values. These changes align with the quantitative data, which show that protein content increased from 0.53 to 3.32% and mean fluorescence rose from 25.92 to 38.68. The moderate response compared to mango and avocado may be explained by the lower baseline protein content and the dominance of carbohydrates (~84% in dehydrated tissue).

The microscopy images demonstrate that dehydration typically enhances protein concentration and fluorescence (avocado, mango, pineapple), but structural and biochemical interactions can override this effect, as observed in papaya. These findings confirm that fluorescence intensity is not merely a function of protein content, but also of protein accessibility, conformational stability, and interactions with the surrounding matrix. Also, confocal microscopy, supported by quantitative image analysis tools such as ImageJ, is a powerful technique for detecting both concentration- and
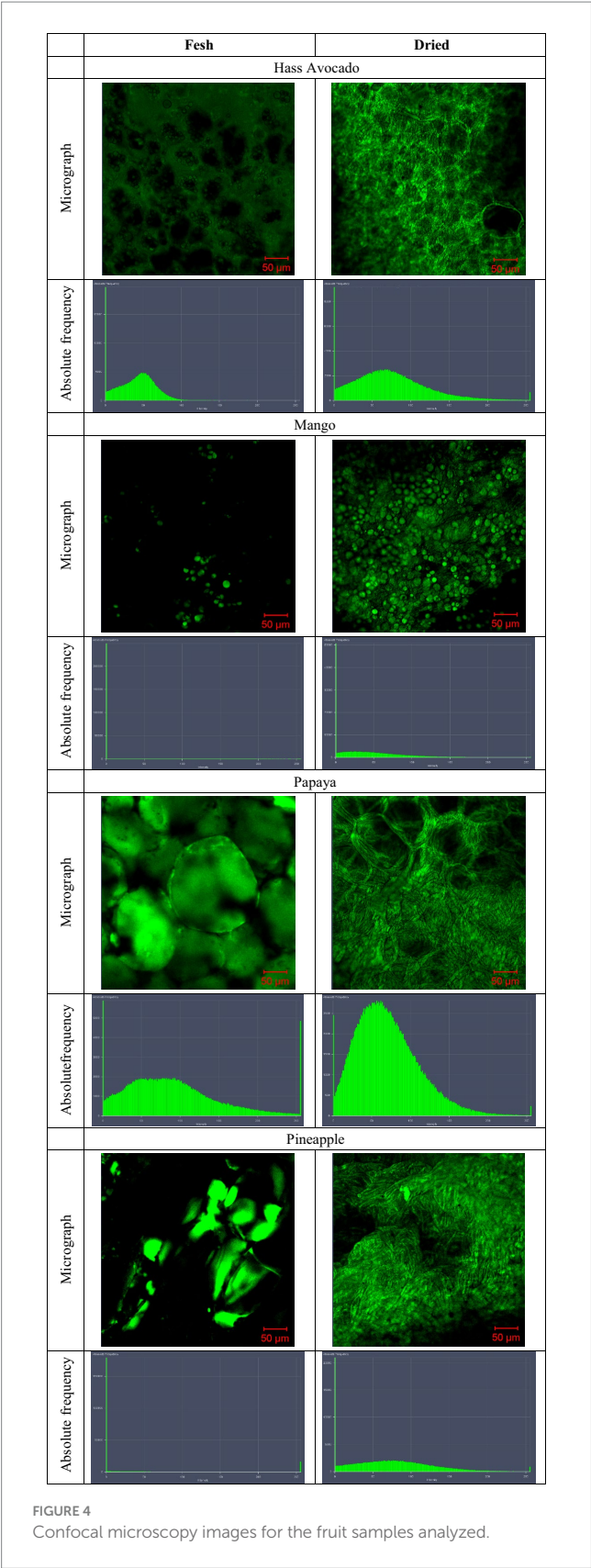
FIGURE 4
Confocal microscopy images for the fruit samples analyzed.

understanding of the effects of dehydration on nutritional and structural integrity.

The dehydration-related fluorescence behavior observed in this study aligns with the typical drying kinetics of fruit matrices, in which moisture loss follows an exponential decay pattern associated with cell wall collapse and the redistribution of soluble compounds. These trends are consistent with classical models such as those of Page and Henderson–Pabis, which describe variations in moisture diffusivity and rate constants during convective drying. Comparable microstructural phenomena have been reported in non-tropical fruits, including apple, persimmon, and kiwi, characterized by cell wall shrinkage, reduction in intercellular porosity, and diminished rehydration capacity after high-temperature dehydration. In this context, the CLSM results for tropical fruits confirm that protein-associated fluorescence variations are closely linked to microstructural integrity, directly influencing texture and water absorption behavior upon rehydration. Overall, dehydration induces complex structural alterations, such as cell wall collapse due to loss of turgor (Aguilera, 2005), formation of microchannels as intercellular spaces disconnect (Chavan et al., 2010), and parenchyma degradation depending on drying conditions (Vilhena et al., 2020), which can be quantitatively described through morphological parameters including porosity, pore diameter, cell sphericity, elongation, and cell wall fraction (Pieczywek et al., 2016).

4 Conclusion

Based on the experimental findings, this study provides a quantitative and structural interpretation of how convective dehydration modifies the cellular and biochemical organization of tropical fruits.

- Convective dehydration reduced the moisture content from 73–91% (fresh) to below 15% (dried), resulting in solute concentration. Protein content increased in all species on a dry-weight basis (avocado: 2.00% → 6.74%; mango: 0.50% → 2.73%; papaya: 0.61% → 4.90%; pineapple: 0.53% → 3.32%).
- A strong positive correlation ($R^2 > 0.90$) was observed between protein content and fluorescence intensity in avocado, mango, and pineapple. At the same time, papaya showed a 17% decrease in fluorescence despite higher protein levels, indicating conformational limitations likely caused by sugar–protein interactions.
- Proximate analysis confirmed species-specific compositional changes: avocado became a lipid- and protein-dominant matrix (lipids: 15.00% → 50.43%), whereas mango, papaya, and pineapple became carbohydrate-rich (85.53, 79.93, and 84.48%, respectively), influencing the fluorescence response.
- CLSM images revealed dehydration-related structural changes, including cell wall collapse, parenchyma compaction, and porosity reduction (~25–40%), which modify cell geometry and may affect texture and rehydration behavior.
- Three-way ANOVA showed that fruit species significantly affected both fluorescence and protein content ($p < 0.0001$), while temperature had a moderate effect ($p = 0.0112$), and air velocity was not significant.

conformation-driven changes in tropical fruit tissues (Oyinloye and Yoon, 2020). Through combining biochemical assays with high-resolution optical imaging, it is possible to obtain a complete

Data availability statement

The raw data supporting the conclusions of this article will be made available by the authors, without undue reservation.

Author contributions

AE-M: Methodology, Writing – original draft, Investigation. JM-T: Methodology, Resources, Supervision, Formal analysis, Writing – original draft. LM-P: Resources, Writing – original draft, Formal analysis, Methodology, Investigation. RG-L: Conceptualization, Supervision, Formal analysis, Writing – original draft, Writing – review & editing.

Funding

Acknowledgments

Conflict of interest

The authors declare that the research was conducted in the absence of any commercial or financial relationships that could be construed as a potential conflict of interest.

Generative AI statement

The authors declare that no Gen AI was used in the creation of this manuscript.

Any alternative text (alt text) provided alongside figures in this article has been generated by Frontiers with the support of artificial intelligence and reasonable efforts have been made to ensure accuracy, including review by the authors wherever possible. If you identify any issues, please contact us.

Publisher's note

All claims expressed in this article are solely those of the authors and do not necessarily represent those of their affiliated organizations, or those of the publisher, the editors and the reviewers. Any product that may be evaluated in this article, or claim that may be made by its manufacturer, is not guaranteed or endorsed by the publisher.

References

Aguilera, J. M. (2005). Why food microstructure? *J. Food Eng.* 67, 3–11. doi: 10.1016/j.jfoodeng.2004.05.050

Azizan, A., Lee, A. X., Abdul Hamid, N. A., Maulidiani, M., Mediani, A., Abdul Ghafar, S. Z., et al. (2020). Potentially bioactive metabolites from pineapple waste extracts and their antioxidant and α-glucosidase inhibitory activities by 1H NMR. *Foods* 9:173. doi: 10.3390/foods9020173

Baur, F. J., and Ensminger, L. G. (1977). The association of official analytical chemists (AOAC). *J. Am. Oil Chem. Soc.* 54, 171–172. doi: 10.1007/BF02670789

Chavan, U. D., Prabhukhanolkar, A. E., and Pawar, V. D. (2010). Preparation of osmotic dehydrated ripe banana slices. *J. Food Sci. Technol.* 47, 380–386. doi: 10.1007/s13197-010-0063-8

Choudhary, P., Devi, T. B., Tushir, S., Kasana, R. C., and Popatrao, D. S. (2023). Mango seed kernel: a bountiful source of nutritional and bioactive compounds. *Food Bioprocess Technol.* 16, 289–312. doi: 10.1007/s11947-022-02889-y

Fautsch Macías, Y. (2014). Food and agriculture Organization of the United Nations (FAO). Rome: FAO.

Galeano-Díaz, T., Monago-Maraña, O., Martín-Tornero, E., and Martín-Merás, I. D. (2025). Application of fluorescence spectroscopy in fruits and vegetables BT - application of fluorescence spectroscopy in food quality and control. Cham: Springer Nature Switzerland, 251–288.

Heredia, A., and Dominguez, E. (2009). The plant cuticle: a complex lipid barrier between the plant and the environment. An overview BT - counteraction to chemical and biological terrorism in east European countries. Dordrecht: Springer Netherlands, 109–116.

Hongli, Q., Baolong, L., Zhiguo, L., Fideline, T.-M., Boyuan, W., and Yande, L. (2025). Novel technique for measuring the 3D geometric size of fruit cells. *Int. J. Agric. Biol. Eng.* 18, 257–264. doi: 10.25165/j.ijabe.20251803.9581

Li, R., Wang, Y., Li, W., and Shao, Y. (2023). Comparative analyses of ripening, texture properties and cell wall composition in three tropical fruits treated with 1-methylcyclopropene during cold storage. *Horticulturae* 9. doi: 10.3390/horticulturae9020126

Magwaza, L. S., and Tesfay, S. Z. (2015). A review of destructive and non-destructive methods for determining avocado fruit maturity. *Food Bioprocess Technol.* 8, 1995–2011. doi: 10.1007/s11947-015-1568-y

Mohapatra, D., and Mishra, S. (2011). Current trends in drying and dehydration of foods. *Food Eng* 22, 311–353. Available online at: https://www.researchgate.net/publication/287275566_Current_trends_in_drying_and_dehydration_of_foods

Onelli, E., Ghiani, A., Gentili, R., Serra, S., Musacchi, S., and Citterio, S. (2016). Specific changes of exocarp and mesocarp occurring during softening differently affect firmness in melting (MF) and non melting flesh (NMF) fruits. *PLoS One* 10:e0145341. doi: 10.1371/journal.pone.0145341

Ovando-Martínez, M., and González-Aguilar, G. A. (2020). Chapter 31 – Papaya. London: Academic Press, 499–513.

Oyinloye, T. M., and Yoon, W. B. (2020). Effect of freeze-drying on quality and grinding process of food produce: a review. *PRO* 8:354. doi: 10.3390/pr8030354

Panarese, V., Laghi, L., Pisi, A., Tylewicz, U., Rosa, M. D., and Rocculi, P. (2012). Effect of osmotic dehydration on *Actinidia deliciosa* kiwifruit: a combined NMR and ultrastructural study. *Food Chem.* 132, 1706–1712. doi: 10.1016/j.foodchem.2011.06.038

Pawley, J. B. (1995). Handbook of biological confocal microscopy. New York, NY: Springer New York, NY.

Pieczywek, P., Cybulska, J., Dyki, B., Konopacka, D., Mieszczakowska-Frąc, M., and Zdunek, A. (2016). New image analysis method for the estimation of global and spatial changes in fruit microstructure. *Int. Agrophys.* 30, 219–229. doi: 10.1515/intag-2015-0073

Qiang, H. L., Li, B. L., Li, Z. G., Tchuenbou-Magaia, F., Wei, B. Y., and Liu, Y. D. Novel technique for measuring the 3D geometric size of fruit cells. *Int J Agric & Biol Eng,* (2025) 18, 257–264. Available online at: https://ijabe.org/index.php/ijabe/article/view/9581

Rasooli Sharabiani, V., Kaveh, M., Abdi, R., Szymanek, M., and Tanaś, W. (2021). Estimation of moisture ratio for apple drying by convective and microwave methods using artificial neural network modeling. *Sci. Rep.* 11:9155. doi: 10.1038/s41598-021-88270-z

Ratti, C. (2001). Hot air and freeze-drying of high-value foods: a review. *J. Food Eng.* 49, 311–319. doi: 10.1016/S0260-8774(00)00228-4

Sana, M., Farooq, M. U., Hassan, S., and Khan, A. (2025). On the machine learning algorithm combined evolutionary optimization to understand different tool designs' wear mechanisms and other machinability metrics during dry turning of D2 steel. *Results Eng.* 25:103998. doi: 10.1016/j.rineng.2025.103998

Sando, T., Hayashi, T., Takeda, T., Akiyama, Y., Nakazawa, Y., Fukusaki, E., et al. (2009). Histochemical study of detailed laticifer structure and rubber biosynthesis-related protein localization in *Hevea brasiliensis* using spectral confocal laser scanning microscopy. *Planta* 230, 215–225. doi: 10.1007/s00425-009-0936-0

Schaffer, B. A., Wolstenholme, B. N., and Whiley, A. W. (2013). The avocado: Botany, production and uses. In CAB books. New York, NY: CABI.

Tejeda-Miramontes, J. P., González-Frías, S. E., Padlon-Manjarrez, S., García-Cayuela, T., Tejada-Ortigoza, V., and Garcia-Amezquita, L. E. (2024). Obtaining a fiber-rich ingredient from blueberry pomace through convective drying: process modeling and its impact on techno-functional and bioactive properties. *LWT* 210:116862. doi: 10.1016/j.lwt.2024.116862

Terai, T., and Nagano, T. (2008). Fluorescent probes for bioimaging applications. *Curr. Opin. Chem. Biol.* 12, 515–521. doi: 10.1016/j.cbpa.2008.08.007

Vega-Gálvez, A., Uribe, E., Poblete, J., García, V., Pastén, A., Aguilera, L. E., et al. (2021). Comparative study of dehydrated papaya (*Vasconcellea pubescens*) by different drying methods: quality attributes and effects on cells viability. *J. Food Meas. Charact.* 15, 2524–2530. doi: 10.1007/s11694-021-00845-6

Vicente-Flores, M., Güemes-Vera, N., Chanona-Pérez, J. J., Perea-Flores, M. d. J., Arzate-Vázquez, I., Quintero-Lira, A., et al. (2021). Study of cellular architecture and micromechanical properties of cuajilote fruits (*Parmentiera edulis* D.C.) using different microscopy techniques. *Microsc. Res. Tech.* 84, 12–27. doi: 10.1002/jemt.23559

Vilhena, N. Q., Gil, R., Llorca, E., Moraga, G., and Salvador, A. (2020). Physico-chemical and microstructural changes during the drying of persimmon fruit cv. Rojo Brillante harvested in two maturity stages. *Foods* 9:870. doi: 10.3390/foods9070870

Yahia, E. (2011). Postharvest biology and technology of tropical and subtropical fruits. Volume 1. Fundamental issues. New York, NY: Springer.

Zhang, X., Liang, J., Lin, X., Chen, J., and Luo, X. (2025). A comprehensive review on the composition, processing methods, and sustainable utilization of tropical fruit seeds in food industry. *Food Front.* 6, 644–669. doi: 10.1002/fft2.493